2nd URSI AT-RASC, Gran Canaria, 28 May - 1 June 2018

Near-Field Microwave Imaging Using Focused Near-Field Beams: An Approach to Mitigate Undesired Scattering Effects

Nozhan Bayat* and Puyan Mojabi
Electrical and Computer Engineering Department, University of Manitoba, Winnipeg, MB, Canada

Abstract

We discuss the use of focused near-field (NF) distributions to irradiate the object of interest in NF microwave imaging. This is pursued with the aim of suppressing the effect of undesired scatterers, which could then lead to the use of simpler inversion algorithms dealing with fewer unknowns. To this end, we investigate the use of an existing NF plate, which is capable of focusing the NF distribution to a subwavelength line (one-dimensional) focus. Similarly, we investigate the same concept, i.e., suppressing the effect of undesired scatterers, using an existing Bessel beam launcher to create a confined NF distribution in free space.

1 Introduction

Microwave imaging (MWI) is an imaging technique using which we can obtain the dielectric profile (and/or magnetic profile) of the object of interest (OI) in a non-destructive fashion. This imaging tool can be (potentially) used in several applications such as biomedical imaging and industrial non-destructive testing [1–8]. In MWI, the OI is illuminated by incident electromagnetic waves. Due to the presence of the OI within the imaging domain, scattered fields will arise which will then be collected by a set of receiving antennas located outside of the OI. This collected data is calibrated and inverted by the use of an appropriate electromagnetic inversion algorithm to reconstruct the (quantitative) image of the OI's complex permittivity profile. This image can then be used for diagnostic applications. MWI can be performed in both time domain and frequency domain, and also in near-field (NF) or far-field zones. In this paper, we consider NF frequency-domain MWI in which the OI resides in the NF zones of the antennas and is irradiated by time-harmonic microwaves.

2 Motivation

Since MWI systems and actual OIs are, in fact, three dimensional (3D) structures, researchers have developed 3D full-vectorial nonlinear inversion algorithms, e.g., see [9]. The use of full-vectorial 3D non-linear inversion algorithms results in increasing the number of unknowns as compared to simpler 3D scalar, 2D, and 1D inversion algorithms. To invert these many unknowns in full-vectorial inversion, we need to collect "sufficient" data from the OI in a 3D imaging chamber. (In the presentation, this topic will be further discussed based on the relation between the MWI problem and the required sampling resolution in near-field antenna measurement systems [10].) In some applications, due to the physical size of the antennas and other practical considerations, it might not be possible to collect sufficient scattering information. This could then result in a significant imbalance between the number of unknown and known quantities in the utilized inversion algorithm. In such cases (i.e., when collecting sufficient data is not practical), the use of simpler inversion algorithms (e.g., 2D inversion algorithms) might be a better option as it reduces the number of unknowns. (For example, in the case of 2D transverse magnetic inversion, the unknowns will be one electric field component and a dielectric contrast in each pixel within the cross-section to be imaged compared to three unknown electric field components and a dielectric contrast in each voxel in 3D full-vectorial inversion.) On the other hand, the use of such simpler inversion algorithms comes with one disadvantage: the resulting 3D effects, which are not modelled in the algorithm, contributes toward the modelling error, thus, degrading the *overall* signal-to-noise ratio (SNR) of the inversion process. In other words, such 3D effects in a 2D inversion scenario are considered as undesired scattering effects, which need to be minimized. To benefit from the advantage of simpler inversion algorithms and at the same time minimize these undesired scattering effects, one might tailor the incident NF so that these undesired scattering effects are reduced. In other words, the incident NF is not only used to interrogate the OI, but is also shaped to justify the use of simpler inversion algorithms. (There are different ways to tailor the incident NF distribution, e.g., by the use of electromagnetic metasurfaces [11].) For example, in [12], we have discussed that it is desirable to use an incident NF that is focused in the elevation plane for 2D scalar inversion. Further investigation of this topic, using a NF plate and a Bessel beam launcher, is the focus of this paper. (We have performed a preliminary investigation of the use of Bessel beams in [13].)

3 Methodology and Results

To evaluate the proposed approach, we first begin by considering a NF plate, as originally introduced in [14], to in-

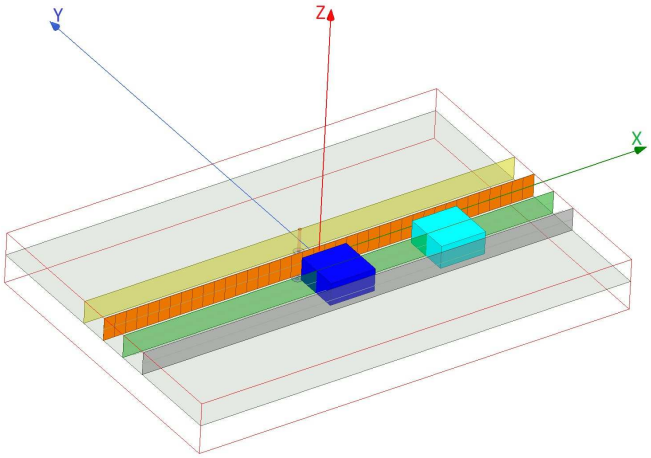

Figure 1. The NF plate (orange plane), introduced in [14], is excited from the yellow plane, and then generates a focused incident NF. The green and grey planes show the focal plane (plane containing the maximum focusing level in the absence of the objects) and the receivers' plane respectively. The dark blue box ($\lambda/10 \times \lambda/10 \times \lambda/20$) which is located at the center represents the object of interest whereas the light blue box (same size and properties as the other box) at the side of the chamber represents the undesired scatterer.

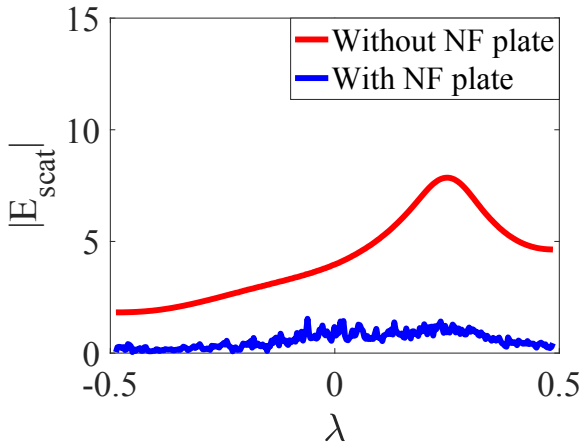

Figure 2. The magnitude of the collected scattered field data at the receivers' locations (placed on the grey plane shown in Figure 1) when we have only the undesired scatterer (light blue box in Figure 1). The blue and red curves are the scattered field data when the NF plate is present and absent respectively.

terrogate the OI with a focused NF beam. The NF plate is a planar structure (the orange plane depicted in Figure 1) that operates in a parallel plate waveguide environment and can provide a line (one-dimensional) focus NF distribution on the focal plane (the green plane shown in Figure 1) once being illuminated by the impinging cylindrical waves. The exciting cylindrical waves are generated by the inner conductor of the coaxial cable which lies on the excitation plane (the yellow plane shown in Figure 1). Several simulation case studies have been performed by using the configuration depicted in Figure 1. (The result of one case study is only shown here.) For all of our case studies, we utilized two types of incident NF distributions: (*i*) a focused NF when the NF plate is present and (*ii*) a non-focused one when the NF plate is absent. Also, for our case studies, we consider two dielectric objects: (1) the dark blue box in Figure 1 that is our OI, and (2) the light blue box in Figure 1 that acts as the undesired scatterer. As can be seen, the dark blue box is positioned centered with respect to the NF plate and the light blue box is placed $\lambda/4$ away from the center. Both of these boxes have the same relative permittivity of 1.5 and the same dimensions of $\lambda/10 \times \lambda/10 \times \lambda/20$. (It should be noted that the parallel plate waveguide is filled with air which serves as the background medium; i.e., the contrast of both the OI and undesired scatterer with respect to the background medium is 0.5).

Let us consider the case when we only have the undesired scatterer; i.e., the dark blue dielectric box shown in Figure 1 has now been removed. In this case study, we compare the collected scattered data at the receivers' locations, which reside on the horizontal line along and parallel to the NF plate on the grey plane shown in Figure 1 under two types of incident NF distributions: when the NF plate is present and when it is absent. The obtained results from this case study has been depicted in Figure 2 where the blue curve represents the magnitude of the collected scattered data at the receivers' locations when the NF plate is present and the red curve shows the magnitude of the collected scattered data when the NF plate has been removed. As can be seen from Figure 2, the undersired scatterer is more "invisible" (smaller scattered fields) when we have utilized the NF plate. In other words, the use of this incident NF enables us to use a smaller imaging domain, thus, reducing the number of unknowns. (The proposed idea has been also investigated through some other simulation studies using this system which will be presented at the conference.)

To study the achievable reconstruction accuracy, we have considered a simple inversion algorithm which is equipped with a calibration technique. (This simple inversion algorithm whose details are to be presented at the conference is a linearized algorithm similar to the Born appproximation.) When the NF plate was present, the reconstructed dielectric value for the OI (dark blue box) was similar in the presence and absence of the undesired scatterer (light blue box). This is expected based on our observation above shown in Figure 2. In particular, for an OI of the relative permittivity of 1.7, the reconstructed values in the presence and absence of the undesired scatterer (having the same dielectric property) were 1.65 - j0.03 and 1.66 - j0.01 respectively for a calibration object with relative permittivity of 1.5. However, when the NF plate was removed, the reconstructed dielectric values for the OI were more sensitive to the presence and ab-

sence of the undesired scatterer. From an information point of view, this means that if the NF plate is absent (i.e., when the incident NF beam is wider), the imaging domain needs to be expanded to include the undesired scatterer as well, thus, resulting in the increase of the number of unknowns.

To further investigate the proposed idea, we have also used a Bessel beam launcher, as introduced in [15], that can create a spot (two-dimensional) focus incident NF distribution, which is maintained over a certain distance away from the launcher. The obtained preliminary results from this launcher will be shown at the conference; these suggest that using the Bessel beam launcher can potentially reduce undesired 3D scattering effects. Further investigation is necessary to conclude whether the achievable reconstruction accuracy can benefit from the use of this launcher.

4 Conclusion

In this paper, we have demonstrated that the effect of undesired scatterers in NF microwave imaging can be reduced by the use of focused incident NF distributions. We have also discussed that an appropriate choice of incident NF can make simpler inversion algorithms more realistic. In particular, this is important when collecting "sufficient" scattering data points is not practical due to hardware challenges, cost issue, or data collection speed. On a more general note, this paper is proposing that the choice of the incident NF can be used as a degree of freedom in the design of NF microwave imaging systems to make the inversion process simpler (and, potentially more accurate).

Acknowledgment

We would like to thank the Canadian Microelectronics Corporation (CMC) for the provision of ANSYS Campus Solution, NSERC of Canada, and the University of Manitoba's GETS Program and UMGF for their financial supports.

References

[1] E. C. Fear, S. C. Hagness, P. M. Meaney, M. Okoniewski, and M. A. Stuchly, "Enhancing breast tumor detection with near-field imaging," *IEEE Microwave Mag.*, vol. 3, no. 1, pp. 48–56, Mar 2002.

[2] M. Persson, A. Fhager, H. D. Trefná, Y. Yu, T. McKelvey, G. Pegenius, J. E. Karlsson, and M. Elam, "Microwave-based stroke diagnosis making global prehospital thrombolytic treatment possible," *IEEE Transactions on Biomedical Engineering*, vol. 61, no. 11, pp. 2806–2817, Nov 2014.

[3] R. Palmeri, M. T. Bevacqua, R. Scapaticci, A. F. Morabito, L. Crocco, and T. Isernia, "Biomedical imaging via wavelet-based regularization and distorted iterated virtual experiments," in *2017 International Conference on Electromagnetics in Advanced Applications (ICEAA)*, Sept 2017, pp. 1381–1384.

[4] M. Hopfer, R. Planas, A. Hamidipour, T. Henriksson, and S. Semenov, "Electromagnetic tomography for detection, differentiation, and monitoring of brain stroke: A virtual data and human head phantom study." *IEEE Antennas and Propagation Magazine*, vol. 59, no. 5, pp. 86–97, Oct 2017.

[5] P. Mojabi and J. LoVetri, "Composite tissue-type and probability image for ultrasound and microwave tomography," *IEEE J. Multiscale and Multiphys. Comput. Techn.*, vol. 1, pp. 26–35, 2016.

[6] Z. Wu and H. Wang, "Microwave tomography for industrial process imaging: Example applications and experimental results." *IEEE Antennas Propag. Mag.*, vol. 59, no. 5, pp. 61–71, Oct 2017.

[7] M. Pastorino, *Microwave Imaging*. New Jersey: John Wiley & Sons, 2010.

[8] N. K. Nikolova, *Introduction to Microwave Imaging*. United Kingdom: Cambridge University Press, 2017.

[9] A. Abubakar and P. M. van den Berg, "Iterative forward and inverse algorithms based on domain integral equations for three–dimensional electric and magnetic objects," *J. Comput. Phys.*, vol. 195, pp. 236–262, 2004.

[10] C. Parini, S. Gregson, J. McCormick, and D. J. van Rensburg, *Theory and Practice of Modern Antenna Range Measurements*. United Kingdom: The Institution of Engineering and Technology, 2014.

[11] A. Epstein and G. V. Eleftheriades, "Huygens' metasurfaces via the equivalence principle: design and applications," *J. Opt. Soc. Am. B*, vol. 33, no. 2, pp. A31–A50, Feb 2016.

[12] N. Bayat and P. Mojabi, "On an antenna design for 2D scalar near-field microwave tomography," *Applied Computational Electromagnetics Society Journal*, vol. 30, pp. 589–598, 2015.

[13] N. Bayat, C. Niu, and P. Mojabi, "Synthetic study of the use of Bessel beam illumination in 2D microwave tomography," in *IEEE APS and USNC-URSI meeting*, Fajardo, Puerto Rico, USA, June 2016.

[14] A. Grbic, L. Jiang, and R. Merlin, "Near-field plates: subdiffraction focusing with patterned surfaces," *Science*, vol. 320, pp. 511–513, 2008.

[15] M. Ettorre and A. Grbic, "Generation of propagating Bessel beams using leaky-wave modes," *IEEE Trans. Antennas Propag.*, vol. 60, no. 8, pp. 3605–3613, Aug 2012.